Preprints of the 21st IFAC World Congress (Virtual)
Berlin, Germany, July 12-17, 2020

Sliding Mode Control with Chattering Attenuation and Hardware Constraints in Spacecraft Applications

M. Mancini [*] **E. Capello** [*,**] **E. Punta** [**]

[*] *Department of Mechanical and Aerospace Engineering Politecnico di Torino, Torino, Italy*

[**] *Institute of Electronics, Computer and Telecommunication Engineering National Research Council of Italy (CNR-IEIIT), Politecnico di Torino, Torino, Italy*

Abstract: Many practical issues should be considered when synthesizing a control system for real applications. In this paper the main objective is the evaluation of the performance of a Sliding Model Controller (SMC) for spacecraft applications, in which implementation issues are included. The key features of the proposed practical design are: (i) chattering attenuation, in which an hyperbolic tangent is considered, and (ii) hardware constraints, in which a reduced SMC update frequency and saturations on the actuation system are included. A comparison between a first order and a super-twisting SMC is performed, including disturbances on the mathematical model. Moreover, computational effort and error accuracy are evaluated for both the strategies, showing the performance of the proposed implementation solutions.

Keywords: Sliding mode control, Control system design, Systems with saturation, Autonomous systems, Non-Linear Control Systems Tracking

1. INTRODUCTION

Many practical issues can arise when control systems are synthesized for real applications. Some of these issues, which are usually considered, are related to external disturbances and hardware constraints, in particular due to limitations of the actuation system. One of the objective of this paper is to evaluate the performance of a practical control system for unmanned spacecraft in orbital servicing mission. The focus of this research is the design of a robust on-board software: this flight software has to be designed to manage unexpected events, such as environment disturbances and noise, and/or crossing of small objects. The proposed control approaches are designed to be as close as possible to "flyable" format, as required by EASA standards (Jones et al., 2002).

The proposed algorithms are characterized by the following key features: (i) low computational effort, (ii) low fuel consumption, and (iii) high safety and robustness. Due to the presence of uncertainties and dynamical constraints, attitude control of a spacecraft must ensure high accuracy and excellent robustness against external disturbances and parameter variations with simple design. Some hardware constraints, such as limited updating frequency of both guidance and control algorithms, have to be included. For this reason, in this paper, sliding mode controllers (SMC) are proposed for the precise attitude control of a spacecraft, since the SMC systems are particularly interesting methodologies, suitable for harsh conditions, such as the space environment, and able to handle external disturbances and uncertainties. Indeed, SMC, (Utkin, 1992; Shtessel et al., 2014), are nonlinear control techniques with remarkable properties of precision, robustness and ease of design, tuning, and implementation. In the last five years, some researches based on SMC systems are proposed for space maneuvers. In (Feng et al., 2016) an optimal SMC strategy combined with a guidance algorithm is proposed for a space maneuver, including external disturbances and obstacle avoidance strategy. In a similar way, in (Li et al., 2018), external disturbances are described for a docking maneuver. Instead, in (Wan et al., 2017), besides external disturbances, actuation constraints are also included for a rendezvous mission. Moreover, in general, actuator saturation is a constraint that exists in almost all the mechanic systems. Thus, input saturation and its time-varying features also deserve special attentions when designing the aerospace control systems.

In our paper, combined with actuation limitations, we include the limited computational power of the on-board systems, considering low update frequency of the controller. As described in (Elmali and Olgac, 1996), the sampling speed is one issue to take into account, since the accuracy of the proposed strategy is function of the maximum attainable sample frequency. One key aspect of the proposed strategies is to show the error accuracy, in terms of attitude tracking of the spacecraft, even when limited-capacity hardware is available. Both first order and second order SMC strategies are compared, suitably designed for a real spacecraft system. Continuous sliding-mode (SM) algorithms are developed as a means of mitigating the drawbacks of the discontinuous classical SM, such as chattering phenomenon and infinite-time convergence. The chattering phenomenon is attenuated by means of hyperbolic tangent, instead of the *sign* function, key feature of the SMC. Simulations are carried out to show the effectiveness of the proposed solutions, from the prac-

⋆ This work was supported by COOPS, International Bilateral Joint CNR.

tical point of view, and showing the ability of the controllers to handle external disturbances. Moreover, the gains of both the proposed SMC strategies are designed including the actuation limitations. This approach shows that the provided control inputs are not saturated, since the gains are designed including physical constraints. Moreover, the computational effort and the error accuracy are evaluated to show the performance of the proposed strategies, even in presence of hardware constraints and limited update frequency.

The paper is organized as follows. A brief introduction to sliding mode controller is in Section 2. The implementation issues are described in Section 3. The spacecraft application, including the dynamics of the system, is in Section 4. Simulation results are introduced in Section 5. Finally, some concluding remarks are described in Section 6.

Throughout the paper $|\cdot|$ is the Euclidean norm or the induced matrix norm. Moreover, let ρ be a function in μ and γ, then the symbols ρ_μ, $\rho_{\mu\mu}$ and $\rho_{\mu\gamma}$ denote, respectively, the first-order partial derivatives $\dfrac{\partial}{\partial\mu}\rho$, the second-order partial derivatives $\dfrac{\partial^2}{\partial\mu^2}\rho$, and the second-order mixed partial derivatives $\dfrac{\partial^2}{\partial\mu\partial\gamma}\rho$.

In the paper any solution of a differential equation with discontinuous r.h.s. must be interpreted in the Filippov sense, (Filippov, 1988).

2. SLIDING MODE CONTROL

In this section, a general nonlinear uncertain control system is introduced. It is therefore shown under which conditions the control problem for this system can be dealt with SMC and which results can be obtained. The classical SMC, (Utkin, 1992), and the second order SMC Super-Twisting (STW) algorithm, (Levant, 1993), are considered.

Sliding mode is a nonlinear control approach, which is able to ensure high accuracy and excellent robustness against external disturbances and parameter variations with simple design. First order SMCs design discontinuous control laws and guarantee that the sliding manifold is reached (i.e. the sliding output reaches zero). Higher order SMCs can steer to zero the sliding output as well as its higher order time derivatives by means of control laws that can be either continuous or not depending on the implemented SMC. The STW algorithm is a second order SMC and it is a continuous controller, which is able to provide all the main properties of SMC for systems affected by smooth matched uncertainties/disturbances with bounded gradients.

2.1 Control System and Problem Statement

Consider the following uncertain nonlinear control system

$$\dot{x} = a(t,x) + b(t,x)u, \tag{1}$$

where $x \in R$ is the state, $u \in R$ is the control input; $a(t,x) \in R$ and $b(t,x) \in R$ are possibly uncertain, yet bounded term.
The sliding variable $\sigma(t,x) \in R$ is chosen for system (1); σ has relative degree one with respect to the control u.
The relevant sliding surface is defined as follows

$$\sigma(t,x) = 0. \tag{2}$$

Let

$$\dot{\sigma}(t,x) = h(t,x) + g(t,x)u, \tag{3}$$

where $h(t,x) = \sigma_t + \sigma_x a(t,x)$ and $g(t,x) = \sigma_x b(t,x)$.

2.2 First-Order SMC

Consider (3) and assume that positive constants H_M, K_m, and K_M are known such that the following conditions hold

$$|h| \le H_M,\ 0 < K_m \le g \le K_M. \tag{4}$$

The first-order control law can be defined and applied to system (1) according to the following

$$u = -\gamma \mathrm{sgn}(\sigma). \tag{5}$$

where σ is the sliding variable in (2) and the control parameter γ, which corresponds to the modulus U_M of the control signal u, is chosen to satisfy

$$\gamma = U_M \ge \frac{H_M}{K_m} + \varepsilon, \quad \varepsilon > 0. \tag{6}$$

The discontinuous control law (5) guarantees the convergence of σ to zero in a finite time, (Utkin, 1992).

Remark 1. According to (5) u is discontinuous and commutes at infinite frequency with a constant magnitude, that is $|u| = U_M$, (Utkin, 1992).

2.3 Super-Twisting SMC

Consider (3) and assume that positive constants C, U_M, K_m, and K_M are known such that the following conditions hold

$$\begin{aligned} \left|\dot{h}\right| + |\dot{g}|\, U_M \le C, \quad & 0 < K_m \le g \le K_M, \\ \left|\frac{h}{g}\right| \le q U_M, \quad & 0 < q < 1. \end{aligned} \tag{7}$$

The STW control algorithm can be defined and applied to system (1) according to the following

$$\begin{aligned} u &= u_1 + u_2 \\ u_1 &= -\lambda |\sigma|^{\frac{1}{2}} \mathrm{sgn}(\sigma), \\ \dot{u}_2 &= \begin{cases} -u, & |u| > U_M, \\ -\alpha \mathrm{sgn}(\sigma), & |u| \le U_M, \end{cases} \end{aligned} \tag{8}$$

where σ is the sliding variable in (2) and the two control parameters satisfy $K_m\alpha > C$ and the sufficient condition

$$\lambda > \sqrt{\frac{2}{K_m\alpha - C}}\, \frac{(K_m\alpha + C)\, K_M\, (1+q)}{{K_m}^2\, (1-q)}. \tag{9}$$

The STW continuous control law (8) guarantees the convergence of both σ and $\dot{\sigma}$ to zero in a finite time, while the control signal remains such that $|u| \le U_M$, provided its initial value $|u(t_0)| \le U_M$, (Levant, 1993), (Shtessel et al., 2014). The sufficient condition (9) can be made less restrictive, (Davila et al., 2005), (Kumar et al., 2017).

Remark 2. According to (8) both the two components u_1 and u_2 of u are continuous signals. When $|u| \le U_M$ the first time derivative of u_2 is discontinuous, in fact $\dot{u}_2$ commutes at infinite frequency with a constant magnitude, that is $|\dot{u}_2| = \alpha \le U_M$, (Levant, 1993).

3. IMPLEMENTATION ISSUES OF SLIDING MODE CONTROLLERS

As previously said, the objective of this paper is to compare two control laws, based on SMC theory, in terms of "practical" performance: (i) easiness to design, (ii) computational effort and (iii) accuracy. In particular, a first order SMC and a second order SMC, called Super-Twisting, are analyzed. Both controllers are implemented by using the *sign* function, from one side, and the *tanh* function, on the other side. This paper also investigates how the reduced update frequency of the control signal affects the performance, compared to high control frequency.

To show the effectiveness of the implementation solutions, the control laws are applied to a practical case, that is a tracking attitude maneuver of a spacecraft in Low Earth orbit. The reason for this choice is that SMC is a particularly interesting control strategy in space operations. In fact it is suitable to operate in hard conditions, such as the space environment, thanks to its features of less "sensibility" to both bounded external disturbances and uncertainties. Furthermore it requires a low computational effort, so it guarantees a real-time control of complex maneuvers. Instead, the main disadvantage of the SMC is due to *chattering* of the control signal, that degrades the components over time. For this reason, in this paper, extensive simulations are performed to analyze the effectiveness of the proposed method to reduce chattering.

In practical applications of SMC, the so-called chattering phenomenon is experienced. This phenomenon can be described as the occurrence of oscillations in the vicinity of discontinuity surfaces characterized by finite frequency and amplitude. It has been deeply analysed in (Utkin and Lee, 2006), (Levant, 2010) and references cited therein. Furthermore the behavior of variable structure control systems in the vicinity of the discontinuity surfaces need to be studied and analysed, (Bartolini and Zolezzi, 1993), (Bartolini et al., 2007), (Zolezzi, 2008). In general, chattering is a harmful phenomenon that leads to low control accuracy. In particular in mechanical applications this phenomenon implies a high wear of the moving parts for which it is practically destructive. Among the reasons for chattering there are certainly the fast "unmodeled" dynamics (e.g. hidden resonance peaks) neglected in the ideal model of the whole control system. These dynamics with small time constants are usually disregarded in models of actuators and sensors. Chattering is also caused by the use of digital controllers characterized by a finite sampling rate. The ideal sliding mode implies the infinite switching frequency of the control. Digital controllers maintain the control constant during a sampling interval, the control switching frequency can be quite low, (Brogliato et al., 2019), (Du et al., 2019).

In this paper we consider the reaching law approach, (Bartoszewicz, 2015; Leśniewski and Bartoszewicz, 2015), to sliding mode control when the system is affected by disturbances. In (Leśniewski and Bartoszewicz, 2015) the use of the *tanh* is proposed for discrete time systems with uncertain parameters and external disturbances. In (Leśniewski and Bartoszewicz, 2015; Leśniewski and Bartoszewicz, 2015) the authors prove that the reaching law exploiting the *tanh* ensures that the quasi-sliding mode is achieved after finite time, and is enforced for the rest of the control process. In our paper, a comparison of the two reaching laws respectively based on the *sign* and *tanh* functions is proposed and the use of the *tanh* is detailed from the practical point of view. The use of the hyperbolic tangent can be mitigated introducing a constant gain in order to obtain an output as close as possible to the *sign* function, Figure 1.

4. SPACECRAFT APPLICATION

This section provides a mathematical description of the selected system, that is attitude dynamics and kinematics of a spacecraft (Markley and Crassidis, 2014; De Ruiter et al., 2012). The attitude dynamics is described by the Euler's equation

$$\dot{\boldsymbol{\omega}}_B = I_B^{-1}[\boldsymbol{M}_B - \boldsymbol{\omega}_B \times (I_B\boldsymbol{\omega}_B + I_{RW}\boldsymbol{\omega}_{RW})], \tag{10}$$

where $\dot{\boldsymbol{\omega}}_B \in \mathbb{R}^3$ is the vector of the angular accelerations of the spacecraft in a body reference frame, $I_B \in \mathbb{R}^{3,3} = [100\ 0\ 0; 0\ 100\ 0; 0\ 0\ 120]$ kg$\cdot m^2$ is the inertia matrix of the spacecraft, $\boldsymbol{\omega}_{RW} \in \mathbb{R}^3$ and $I_{RW} \in \mathbb{R}^{3,3}$ are related to the actuation system (i.e. reaction wheels). Finally, $\boldsymbol{M}_B \in \mathbb{R}^3$ is the total torque applied to the spacecraft and it consists of two terms

$$\boldsymbol{M}_B = \Delta\boldsymbol{M}_{ex} + \boldsymbol{M}_{RW}, \tag{11}$$

where $\boldsymbol{M}_{RW} \in \mathbb{R}^3$ is the torque provided by the reaction wheels, that represents the spacecraft actuation input provided by the controller, and $\Delta\boldsymbol{M}_{ex} \in \mathbb{R}^3$. In a Low Earth Orbit (LEO), the torque due to orbital external disturbances $\boldsymbol{M}_{ex}$ is mainly due to two contributions. As deeply detailed in (Markley and Crassidis, 2014; Mancini et al., 2020), these effects are: i) a constant moment of about 10^{-5} Nm due to the solar pressure and ii) a term of the order of about 10^{-4} Nm produced by the gravitational effects. For this reason in this paper, these disturbances are modeled as non-constant random values, in the range of $[-10^{-4}, 10^{-4}]$ Nm along the three axes. Instead, the maximum value of the torque that the reaction wheels can exert (i.e. the control authority) is saturated at 0.075 Nm, for the three axes.

In this work, the attitude kinematics of the spacecraft is studied by means of quaternions $q = [q_s, q_{v1}, q_{v2}, q_{v3}]^T \in \mathbb{R}^4$, where q_s is the scalar part of the quaternion, while $q_{v,i}$ for $i = 1 \dots 3$ is the vectorial part. Quaternions are defined as

$$\dot{q} = \tfrac{1}{2}\Sigma(q)\omega_B, \tag{12}$$

where $\Sigma(q) \in \mathbb{R}^{3,4}$ is the quaternion matrix, defined as

$$\Sigma(q) = \begin{bmatrix} q_s I_3 + Q_{13} \\ -q_{v_{13}}^T \end{bmatrix}, \tag{13}$$

where $q_s \in \mathbb{R}$ is the quaternion scalar component, $q_{v_{13}} = [q_{v,1}, q_{v,2}, q_{v,3}]^T \in \mathbb{R}^3$ is the vector of the first three components of the quaternion and $Q_{13} \in \mathbb{R}^{3,3}$ is the skew-symmetric matrix

$$Q_{13} = \begin{bmatrix} 0 & -q_{v,3} & q_{v,2} \\ q_{v,3} & 0 & -q_{v,1} \\ -q_{v,2} & q_{v,1} & 0 \end{bmatrix}.$$

In this paper, quaternions express the orientation of the spacecraft with respect to a frame jointed to the desired attitude, that is $q_d = [1, 0, 0, 0]^T$. The initial orientation of the spacecraft is chosen using a set of Euler angles $[\phi, \theta, \psi]_{t=0} = [10, 15, 5]^T$ (De Ruiter et al., 2012). Then, using a 3-1-3 rotation the initial set of quaternions $q_{t=0}$ is computed. Moreover, for the definition of the sliding surface, the quaternion error is evaluated as in (Wu et al., 2011): $\delta q = q \otimes q_d^{-1}$, where $\otimes$ represent the quaternion multiplication that is defined in (Shuster, 1993). $\delta q \in \mathbb{R}^4$ consists of a scalar part δq_s and a vectorial part $\delta q_{v,i}$ for $i = 1, \dots, 3$. Then, for the evaluation of the sliding surface, only the vectorial part of δq is used, that is $\delta q_{v_{13}} = [\delta q_{v,1}, \delta q_{v,2}, \delta q_{v,3}]^T \in \mathbb{R}^3$.

A scientific targeting maneuver is considered as a reference, this means that the the payload has to point towards the scien-

tific target of interest. Therefore, at the initial step, the spacecraft is affected by an attitude error, which must be steered to zero by the control system. When the zero error is reached, the attitude must be kept constant, to allow the observation of the defined target by the payload.

4.1 First Order SMC

The input $u_\omega \in \mathbb{R}^3$ is defined, as in (Utkin, 1992),

$$u_\omega = -C_\omega \delta\dot{q}_{v_{13}} - \rho_\omega \text{sgn}(\sigma_\omega) \tag{14}$$

where the control parameters $C_\omega \in \mathbb{R}^{3,3}$ positive definite matrix and $\rho_\omega \in \mathbb{R}$ are defined as indicated in (Shtessel et al., 2014), while the vector $\delta\dot{q}_{v_{13}}\mathbb{R}^3$ defines time derivative of the quaternion error. The sliding output for the first order SMC is defined as

$$\sigma_\omega = \omega_B + K_\omega \delta q_{v_{13}} \tag{15}$$

with $K_\omega \in \mathbb{R}^{3,3}$ positive definite matrix, the vector $\delta q_{v_{13}} \in \mathbb{R}^3$ defines the quaternion error, as previously indicated.
As briefly described above, in this work a modified version of (14) is also implemented:

$$u_\omega = -C_\omega \delta\dot{q}_{v_{13}} - \rho_\omega \tanh(k_\sigma \cdot \sigma_\omega) \tag{16}$$

where $k_\sigma \in \mathbb{R}$ is used to mitigate the effect of the *tanh* function, i.e., the highest is k_σ, the most the output of the *tanh* function tends to the output of the *sign* function, as Figure 1 shows.

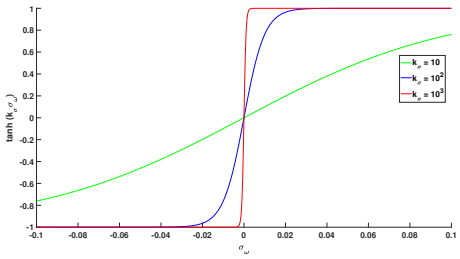

Fig. 1. Effect of k_σ on the *tanh* function

4.2 Super-Twisting SMC

The input $u_\omega\mathbb{R}^3$ is defined in accordance to the STW algorithm, (Levant, 1993), as follows

$$\begin{aligned} u_\omega &= -\lambda|\sigma_\omega|^{\frac{1}{2}}\text{sgn}(\sigma_\omega) + v_\omega\,, \\ \dot{v}_\omega &= \begin{cases} -u_\omega & \text{if } |u_\omega| > U_M\,, \\ -\alpha\text{sgn}(\sigma_\omega) & \text{if } |u_\omega| \le U_M\,, \end{cases} \end{aligned} \tag{17}$$

where the control parameters λ, α, and U_M have to be chosen as specified in (Levant, 1993; Shtessel et al., 2014).

The sliding output for the super-twisting controller is defined as

$$\sigma_\omega = \omega_B + K_\omega \delta q_{v_{13}} \tag{18}$$

with $K_\omega \in \mathbb{R}^{3,3}$ positive definite matrix and, as previously details, the vector $\delta q_{v_{13}}$ defines the quaternion error.
As for the First Order SMC, the STW SMC is also implemented using the *tanh* function in Eq. (17). So we have

$$\begin{aligned} u_\omega &= -\lambda|\sigma_\omega|^{\frac{1}{2}}\tanh k_\sigma(\sigma_\omega) + v_\omega\,, \\ \dot{v}_\omega &= \begin{cases} -u_\omega & \text{if } |u_\omega| > U_M \\ -\alpha\tanh k_\sigma(\sigma_\omega) & \text{if } |u_\omega| \le U_M \end{cases}. \end{aligned} \tag{19}$$

5. SIMULATION RESULTS

Extensive simulations are performed through *Matlab* software to analyze the effectiveness of the proposed control laws in driving to zero the quaternion error. Both control systems are implemented and compared in terms of time required for the attitude to converge to the desired one (T_{conv}), chattering of the command signal, final error in terms of quaternions. Moreover, the control effort, which represents a power consumption estimation, is evaluated as $CE = \sum_{k=0}^{T_{conv}} \|H_{RWk}\|\Delta t$, where $\|H_{RWk}\| = \sqrt{H_{RWkx}^2 + H_{RWky}^2 + H_{RWkz}^2}$ and Δt is the sample time of the simulation. As regards T_{conv}, it is taken as the time at which the error in terms of quaternions is $\|[\delta q_{v,1}, \delta q_{v,2}, \delta q_{v,3}]^T\| < 10^{-4}$.
The following cases and combinations of simulations are considered

a. Order of the SMC: First Order and STW.
b. Function used in the control law: *sign* and *tanh*.
c. Update frequency: $f = 5\ Hz$ and $f = 1000\ Hz$.

With all the combinations, 8 different cases are studied. In the next section, only the most significant results are presented.

5.1 Comparison between STW SMC vs First Order SMC

Fig. 2 shows that STW provides a smoother control signal than the First Order-SMC. This behavior can be especially observed in case of using the *sign* function. In fact, the blue band in the left part of Fig. 2 represents the chattering of the input signal in this case. Furthermore, the First Order SMC with the *sign* function provides a discontinuous control, so it does not fit well with reaction wheels, that exert a continuous torque. The zoom, in the box of Fig. 2, shows that STW reduces the chattering of the input signal, even when the *tanh* function is used.

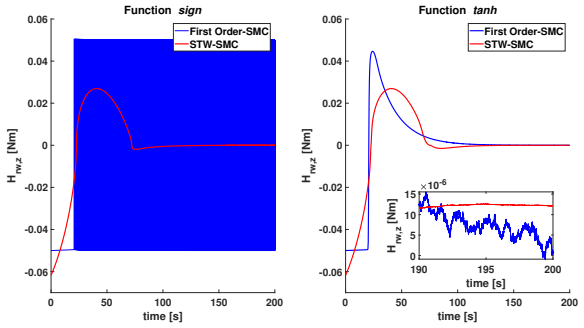

Fig. 2. Comparison of the torque around Z_{body} required by the different control laws, i.e., First Order SMC and STW SMC. ($f = 10^3\ Hz$)

Finally, in Table 1 First Order SMC and STW are compared on the basis of the merit parameters previously mentioned, with an update frequency of $f = 10^3\ Hz$. As evident, the STW controller reaches the desired attitude more accurately, more quickly and with a lower power consumption than the First Order SMC.

Table 1. Performance Indicators for First Order and STW SMC with *sign* function. ($f = 10^3\ Hz$)

Order of SMC	T_{conv}	Final Quaternion Error	Control Effort
First Order	161 s	$1.456 \cdot 10^{-5}$	15.89 Nms
STW SMC	144 s	$6.194 \cdot 10^{-6}$	2.54 Nms

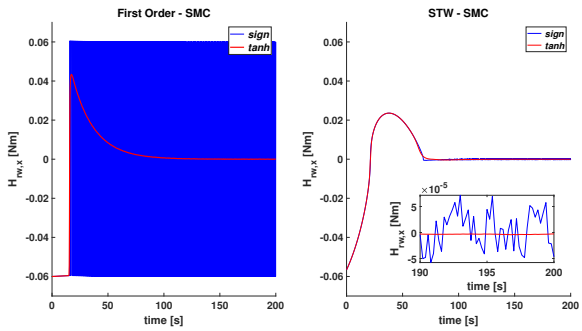

Fig. 3. Comparison of the torque around X_{body} required when *sign* or *tanh* function are used. ($f = 5\ Hz$)

5.2 Comparison between tanh vs sign

Fig. 4 shows that by using the *tanh* function rather than the *sign* function in the control law, the chattering of the input signal is reduced. This effect can be observed in particular for the First Order SMC. Nevertheless, even in the STW SMC, the use of the *tanh* function is able to smooth the control action, more than the *sign* function, as in the zoom of Fig. 4.

In Table 2 the performance of only the STW SMC are analyzed for an update frequency of $f = 5\ Hz$. In particular, this Table provides a comparison of cases where *tanh* function or *sign* function is implemented. Results shows that when the *tanh* is used, the controller reaches the desired attitude more quickly and with a lower power consumption, but the accuracy on the final attitude is greater when the control law uses the *sign* function. From the practical point of view, the error accuracy obtained with the *tanh* is very good for precise pointing maneuvers.

Table 2. Performance Indicators for STW SMC with *sign* and *tanh* function. ($f = 5\ Hz$)

Function used	T_{conv}	Final Quaternion Error	Control Effort
sign	144 s	$5.853 \cdot 10^{-6}$	2.55 Nms
tanh	115 s	$2.290 \cdot 10^{-5}$	2.52 Nms

5.3 Comparison with a Linear Quadratic Regulator

A comparison with a Linear Quadratic Regulator (LQR) is included, considering as update frequency of the controller 5 Hz, as in the previous Section. LQR control system is widely used in real space mission as, for example, in (Guarnaccia et al., 2016). The task of the control function is to provide an input to the reaction wheels, including the effects of disturbances and errors. For the design of an LQR, a linearized dynamic model needs to be considered, in which gyroscopic torque due to RW is neglected, as detailed in (Dentis et al., 2016).

5.4 Comparison 5 Hz vs 1000 Hz

Fig. 5 provides a comparison of the torque around Y_{body}, assigned by the STW SMC, when the update frequency is $f = 5\ Hz$ or $f = 1000\ Hz$. We can notice that by increasing the update frequency the chattering is reduced, especially when the *sign* function is used. Note that, in an "ideal" SMC, the frequency of the controller is close to infinity, which is not available in a real system.

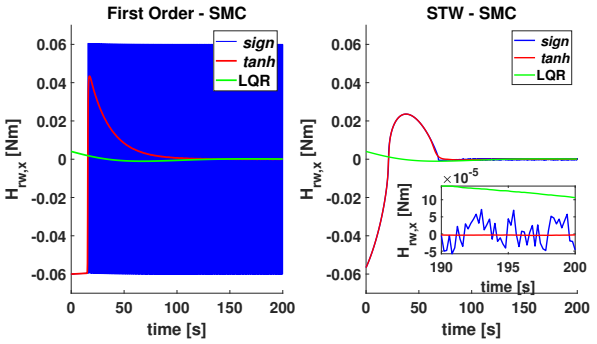

Fig. 4. Comparison of the torque around X_{body} with LQR and SMC. ($f = 5\ Hz$)

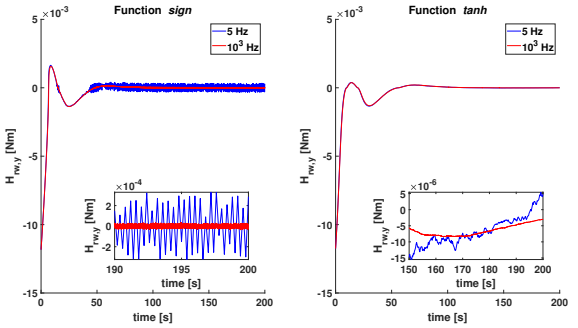

Fig. 5. Comparison of the torque around Y_{body} required by the STW SMC with sample time $f = 5\ Hz$ and $f = 1000\ Hz$

More results related to the effect of the update frequency f are provided in Tables 3 and 4. In particular, the performances of both the control strategy First Order SMC and STW SMC with *tanh* function are evaluated with $f = 5\ Hz$ and and $f = 10^3\ Hz$. We can observe that the obtained results in terms of accuracy and control effort are quite the same. This means that, for the selected first and second order SMC, by using the *tanh* function, high frequency of update is not required to obtain the desired performance.

Table 3. Performance Indicators for STW SMC with *tanh* function, $f = 5\ Hz$ and $f = 10^3\ Hz$.

Update Frequency	T_{conv}	Final Quaternion Error	Control Effort
5 Hz	115 s	$2.290 \cdot 10^{-5}$	2.52 Nms
10^3 Hz	115 s	$2.068 \cdot 10^{-5}$	2.52 Nms

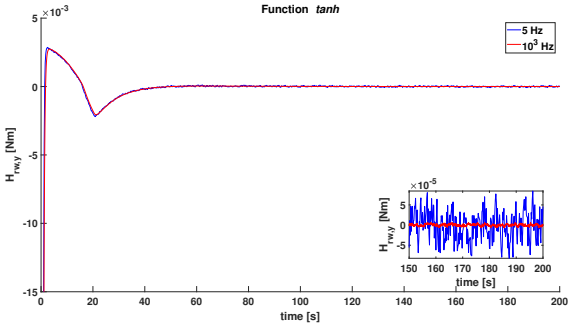

Fig. 6. Comparison of the torque around Y_{body} required by the First Order SMC with sample time $f = 5\ Hz$ and $f = 1000\ Hz$

Table 4. Performance Indicators for First Order SMC with *tanh* function, $f = 5\ Hz$ and $f = 10^3\ Hz$.

Update Frequency	T_{conv}	Final Quaternion Error	Control Effort
5 Hz	159 s	$1.231 \cdot 10^{-5}$s	2.81 Nms
10^3 Hz	158 s	$1.183 \cdot 10^{-5}$	2.52 Nms

6. CONCLUSION

Practical issues can arise when control systems are synthesized for real applications, usually related to external disturbances and hardware constraints, in particular due to limitation of the actuation system. In this paper, implementation of Sliding Mode Control (SMC) strategies for a spacecraft application are proposed, in which some practical issues are included: (i) actuation and frequency constraints (due to the on-board hardware) and (ii) chattering attenuation, via mathematical function (i.e. hyperbolic tangent). The effectiveness of the proposed solutions are shown in terms of avoidance of input saturation, low computational effort and error accuracy. Future works will include adaptation of the second order sliding mode, estimation of parameters and evaluation of the measurement noise.

REFERENCES

Bartolini, G., Punta, E., and Zolezzi, T. (2007). Approximability properties for second-order sliding mode control systems. *IEEE Trans. Automatic Control*, 52(10), 1813–1825.

Bartolini, G. and Zolezzi, T. (1993). Behavior of variable — structure control systems near the sliding manifold. *Systems & Control Letters*, 21, 43–48.

Bartoszewicz, A. (2015). A new reaching law for sliding mode control of continuous time systems with constraints. *Transactions of the Institute of Measurement and Control*, 37(4), 515–521.

Brogliato, B., Polyakov, A., and Efimov, D. (2019). The implicit discretization of the super-twisting sliding-mode control algorithm. *IEEE Trans. Automatic Control*. doi: 10.1109/TAC.2019.2953091.

Davila, J., Fridman, L., and Levant, A. (2005). Second-order sliding-mode observer for mechanical systems. *IEEE Trans. Automatic Control*, 50(11), 1785–1789.

De Ruiter, A.H., Damaren, C., and Forbes, J.R. (2012). *Spacecraft dynamics and control: an introduction*. John Wiley & Sons.

Dentis, M., Capello, E., and Guglieri, G. (2016). A novel concept for guidance and control of spacecraft orbital maneuvers. *International Journal of Aerospace Engineering*, 2016.

Du, H., Zhai, J., Chen, M., and Zhu, W. (2019). Robustness analysis of a continuous higher order finite-time control system under sampled-data control. *IEEE Trans. Automatic Control*, 64(6), 2488—-2494.

Elmali, H. and Olgac, N. (1996). Implementation of sliding mode control with perturbation estimation (smcpe). *IEEE Transactions on Control Systems Technology*, 4(1), 79–85. doi:10.1109/87.481770.

Feng, L., Ni, Q., Bai, Y., Chen, X., and Zhao, Y. (2016). Optimal sliding mode control for spacecraft rendezvous with collision avoidance. In *2016 IEEE Congress on Evolutionary Computation (CEC)*, 2661–2668. doi:10.1109/CEC.2016.7744122.

Filippov, A.F. (1988). *Differential Equations with Discontinuous Right-Hand Sides*. Kluwer.

Guarnaccia, L., Bevilacqua, R., and Pastorelli, S.P. (2016). Suboptimal lqr-based spacecraft full motion control: Theory and experimentation. *Acta Astronautica*, 122, 114 – 136. doi:https://doi.org/10.1016/j.actaastro.2016.01.016. URL http://www.sciencedirect.com/science/article/pii/S0094576516000266.

Jones, M., Gomez, E., Mantineo, A., and Mortensen, U.K. (2002). Introducing ecss software-engineering standards within esa. *EASA bulletin*.

Kumar, P.R., Behera, A.K., and Bandyopadhyay, B. (2017). Robust finite-time tracking of stewart platform: A super-twisting like observer-based forward kinematics solution. *IEEE Trans. on Industrial Electronics*, 64(5), 3776–3785.

Levant, A. (1993). Sliding order and sliding accuracy in sliding mode control. *International journal of control*, 58(6), 1247–1263.

Levant, A. (2010). Chattering analysis. *IEEE Trans. Automatic Control*, 55(6), 1380—-1389.

Leśniewski, P. and Bartoszewicz, A. (2015). Hyperbolic tangent based switching reaching law for discrete time sliding mode control of dynamical systems. In *2015 International Workshop on Recent Advances in Sliding Modes (RASM)*, 1–6. doi:10.1109/RASM.2015.7154589.

Leśniewski, P. and Bartoszewicz, A. (2015). A new class of non-linear reaching laws for sliding mode control of discrete time systems. In *Recent Advances in Sliding Modes: From Control to Intelligent Mechatronics*, 99–128. Springer.

Li, Q., Yuan, J., and Wang, H. (2018). Sliding mode control for autonomous spacecraft rendezvous with collision avoidance. *Acta Astronautica*, 151, 743–751.

Mancini, M., Bloise, N., Capello, E., and Punta, E. (2020). Sliding mode control techniques and artificial potential field for dynamic collision avoidance in rendezvous maneuvers. *IEEE Control Systems Letters*, 4(2), 313–318. doi:10.1109/LCSYS.2019.2926053.

Markley, F.L. and Crassidis, J.L. (2014). *Fundamentals of spacecraft attitude determination and control*, volume 33. Springer.

Shtessel, Y., Edwards, C., Fridman, L., and Levant, A. (2014). *Sliding mode control and observation*. Springer Science+Business Media, New York.

Shuster, M.D. (1993). A survey of attitude representations. *Navigation*, 8(9), 439–517.

Utkin, V. and Lee, H. (2006). Chattering analysis. In C. Edwards, C. Fossas, and L. Fridman (eds.), *Advances in Variable Structure and Sliding Mode Control*, volume 334 of *Lecture Notes in Control and Information Sciences*, 107–123. Berlin, Germany: Springer Verlag.

Utkin, V.I. (1992). *Sliding modes in optimization and control problems*. Springer Verlag, New York.

Wan, N., Naidu, D.S., Liu, M., Wu, L., and Weiran Yao (2017). Adaptive sliding mode control for spacecraft rendezvous in near-circular orbits with time-varying saturation constraint. In *2017 American Control Conference (ACC)*, 5812–5817. doi:10.23919/ACC.2017.7963861.

Wu, S., Radice, G., Gao, Y., and Sun, Z. (2011). Quaternion-based finite time control for spacecraft attitude tracking. *Acta Astronautica*, 69(1), 48 – 58. doi:https://doi.org/10.1016/j.actaastro.2011.03.001. URL http://www.sciencedirect.com/science/article/pii/S0094576511000580.

Zolezzi, T. (2008). Real states of stable sliding mode control systems. *Systems & Control Letters*, 57, 778–783.